

# HADIS: Hybrid Adaptive Diffusion Model Serving for Efficient Text-to-Image Generation

Qizheng Yang  
University of Massachusetts Amherst  
Amherst, MA, USA  
qizhengyang@umass.edu

Tung-I Chen  
University of Massachusetts Amherst  
Amherst, MA, USA  
tungichen@umass.edu

Siyu Zhao  
University of Massachusetts Amherst  
Amherst, MA, USA  
siyuzhao@umass.edu

Ramesh K. Sitaraman  
University of Massachusetts Amherst  
Amherst, MA, USA  
ramesh@cs.umass.edu

Hui Guan  
University of Massachusetts Amherst  
Amherst, MA, USA  
huiguan@cs.umass.edu

## Abstract

Text-to-image diffusion models have achieved remarkable visual quality but incur high computational costs, making real-time, scalable deployment challenging. Existing query-aware serving systems mitigate the cost by cascading lightweight and heavyweight models, but most rely on a fixed cascade configuration and route all prompts through an initial lightweight stage, wasting resources on complex queries. We present HADIS, a hybrid adaptive diffusion model serving system that jointly optimizes cascade model selection, query routing, and resource allocation. HADIS employs a rule-based prompt router to send clearly hard queries directly to heavyweight models, bypassing the overhead of the lightweight stage. To reduce the complexity of resource management, HADIS uses an offline profiling phase to produce a Pareto-optimal cascade configuration table. At runtime, HADIS selects the best cascade configuration and GPU allocation given latency and workload constraints. Empirical evaluations on real-world traces demonstrate that HADIS improves response quality by up to 35% while reducing latency violation rates by 2.7-45× compared to state-of-the-art model serving systems.

## 1 Introduction

Text-to-image diffusion models such as Stable Diffusion XL [27], DALL·E3 [24], and the more recent Diffusion Transformer [26] have demonstrated remarkable capabilities in generating semantically rich, high-quality images from natural language prompts. These models power emerging applications in creative design, e-commerce, and content generation, where users expect both realism and responsiveness. However, the computational cost of these models remains a bottleneck: generating a single image often requires multiple seconds of GPU time due to the iterative denoising process, posing significant challenges to real-time and scalable deployments in production model serving systems.

**Model Serving Goals.** A model serving system has two key goals. First, the system must *use resources efficiently* to serve queries (i.e., text prompts from the user) with *high*

*throughput*. Second, since queries are served to users in real time, the system must guarantee *service-level objectives (SLOs)* that require the latency of response to be within a specified threshold, even as user queries vary widely in complexity. Simple queries like “a banana on a white plate” require minimal computation, whereas complex ones like “a surreal cityscape representing time and memory” demand deeper semantic understanding and finer generative detail. Serving all queries with a “heavyweight” model that has a high computational cost leads to excessive resource usage and response latencies, while using a low-cost “lightweight” model alone may compromise the quality of the response. Therefore, a model serving system must dynamically adjust to query arrival rates and query difficulty to satisfy overall throughput and SLO constraints.

**Model Scaling.** Model scaling has emerged as a key approach to designing model serving systems. An initial example of this approach proposed in Proteus [4] introduces the notion of accuracy scaling that uses less-accurate lower-cost “lightweight” models during peak periods when higher throughput is required, while using more accurate higher-cost models at other times. More recently, *query awareness* has been used to enhance model scaling where each query is processed through a *model cascade* that is a set of models sequenced from lighter weight ones to heavier weight ones. Each query is routed sequentially through the models in the cascade till a response of acceptable quality is obtained. DiffServe [5] is an example of such a cascade using two stages: every prompt is first processed by a lightweight model, and the generated image is assessed by a discriminator. If the image is deemed low-quality, the prompt is re-routed to a heavyweight model. The easier queries only require the first stage of the cascades, saving resources and latency, while the harder queries would need to be routed to the second.

**Limitations of Current Solutions.** The current state-of-the-art serving systems using model cascades have two key limitations. First, the models chosen for a cascade may not be optimal for all query workloads. For instance, DiffServe relies on a fixed pair of lightweight and heavyweight models, even

though different workloads and latency budgets may favor different combinations. Second, model cascades inherently increase both resource usage and latency as some fraction of the queries need to get routed through multiple models. For instance, in a two-model cascade, all prompts are sent to a lightweight model, which wastes resources for queries that are hard and require heavyweight processing regardless.

**Our Main Ideas.** These limitations motivate our main ideas which we list below.

(i) *Dynamic choice of models.* As diffusion models proliferate, each variant offers different trade-offs between latency and quality. Statically fixing model combinations in a cascade across all query workload scenarios is inefficient. Therefore, we design a model serving system that dynamically chooses the models in a cascade to suit the properties of the current query workload.

(ii) *Resource-efficient query routing.* Routing each query through the entire model cascade wastes computational resources and increases the latency. For instance, routing the harder queries to a lightweight model is unlikely to produce a response of acceptable quality, leading to a waste of compute resources and an increase in the latency. We propose a *hybrid architecture* shown in Figure 1 that consists of both a *router* and a *discriminator* to reduce resource wastage and latency. Our system begins with a rule-based router that computes a query difficulty score using linguistic and semantic features, including token rarity, abstractness, spatial relations, etc. Queries that are predicted to be hard are routed directly to a heavyweight model, skipping the lightweight model(s) in the cascade. Queries that are classified as easy are processed by a lightweight model, whose outputs are then evaluated by an image discriminator for both semantic and aesthetic quality. If the generated images fail to meet the quality requirements, the query is sent to the heavyweight model. This hybrid design reduces computational overhead and latency for easy queries and avoids wasteful lightweight model inference on hard queries.

(iii) *Managing cascade complexity.* The plethora of diffusion model variants, each offering a different quality-latency tradeoff, raises the possibility of complex model serving architectures consisting of many model variants, discriminators and router components. We show that such complexity is unnecessary and it is sufficient to dynamically choose a simple two-stage model cascade with a single router and discriminator to achieve the benefits of model scaling. This observation greatly reduces the space of architectural choices and enables efficient resource management.

(iv) *Reducing the complexity of resource management.* Resource management of model cascades is a complex NP-hard problem that is often solved using a Mixed-Integer Linear Program (MILP) [5]. While restricting the architecture to two-stage cascades helps, we reduce the combinatorial complexity even further as follows. We use offline profiling to

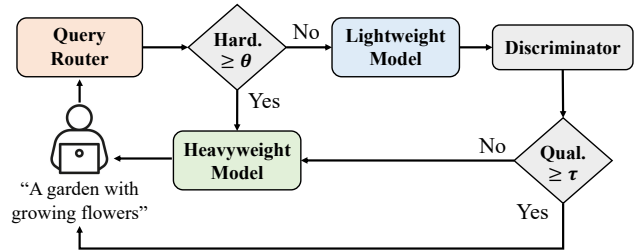


**Figure 1.** Text-to-Image Serving Workflow of HADIS.

benchmark all pairwise model combinations under different routing thresholds and generate a *cascade configuration lookup table*. Each configuration in this table encodes a specific combination of models, thresholds, latency measurements, and the estimated ratio of hard queries (i.e., the percentage of queries that will likely be routed to a heavyweight model given the current threshold). The table prunes the search space by identifying Pareto-optimal configurations that offer the best quality-latency trade-offs. At runtime, the system leverages this table to select a configuration that meets the desired SLO constraints. To determine the optimal deployment strategy given a workload distribution and system constraints (e.g., GPU count, latency budget, etc), we formulate the configuration selection and resource allocation as an MILP problem. This formulation jointly optimizes routing decisions, model assignments, and resource partitioning to maximize overall serving efficiency and quality.

**Our Contributions.** Our specific contributions are below.

- We propose adaptive model cascade selection, dynamically selecting optimal pairwise model cascades based on various workload and latency constraints.
- We propose a hybrid routing strategy consisting of a rule-based query router and a learned image discriminator, jointly reducing computational overhead while preserving response quality.
- We address the complex resource management problem for adaptive model cascade through profiling Pareto-optimal configurations and formalizing it as a mixed integer linear programming (MILP) problem.
- We implement these approaches in a production-ready system, HADIS. Experiments show that it improves response quality by up to 35% and SLO violation by 2.7-45× compared to the latest research prototype.

## 2 Background and Rationale for Design

We discuss the background and rationale for the key design choices made by our model serving system, HADIS.

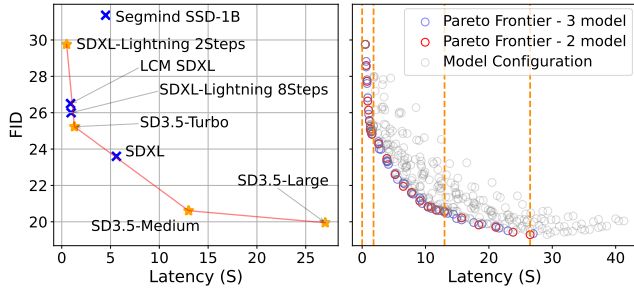


**Figure 2.** Quality-latency tradeoffs of different diffusion model variants (*left*) and model cascades (*right*). Quality is measured by Fréchet Inception Distance [18] (FID, lower is better). The cascades are constructed by the model variants colored in orange in the left panel. The orange dashed lines partition latency into three regimes where each regime has a distinct model cascade that yields the frontier points.

## 2.1 Background for text-to-image diffusion models

Text-to-image diffusion models embody a clear quality-latency trade-off (see Figure 2-*left*): more compute (e.g., deeper networks or transformers, more denoising steps, etc) typically yields better image quality but longer runtime (and latency) and lesser throughput (i.e., fewer queries processed per second). In our setting on L40S GPUs, the spectrum spans sub-second generation (e.g., SDXL-Lightning at 2 steps  $\approx 0.5$ s) to tens of seconds (e.g., SD3.5-Large at 50 steps  $\approx 27$ s) for an image of  $1024 \times 1024$  resolution.

Prior query-aware model serving approaches [5, 8] route queries via a cascade to optimize throughput and SLO violation ratios. In the case of a simple two-model cascade, the first model could be a lightweight model that offers low latency and relatively low quality, and the second model could have higher latency and quality. A discriminator decides if the output of the first model is of sufficiently high quality, failing which the query is routed to the second model of the cascade. This reduces average latency relative to always using a heavyweight model, but still incurs a non-trivial overhead since every query incurs the overhead of the first lightweight model. Further, a longer cascade with more than two models could incur more computational and latency overheads as some queries would pass through all models in the cascade to produce a response.

## 2.2 Rationale for two-model cascades

We show that two-model cascades offer comparable quality-latency trade-offs as model cascades with more model variants. Figure 2-*right* explores the design space of diffusion-model cascades using four model variants (orange stars in the left panel). For each candidate cascade we enumerate routing policies specified by the fraction of queries routed to the heavyweight model(s), and measure the resulting mean latency (x-axis) and FID (y-axis) on 5k prompts. The right

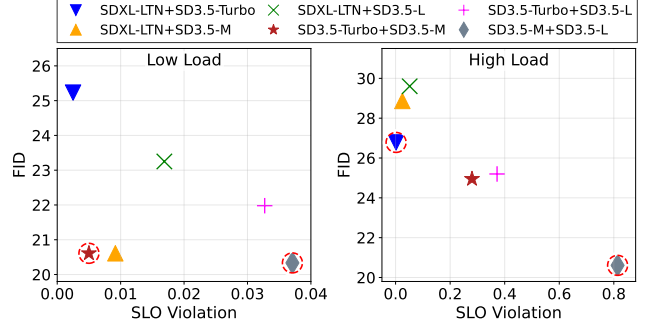


**Figure 3.** Limitations of fixed model cascades. In both panels, each point represents a distinct two-model cascade. Comparing between low load (*left*) and high load (*right*), the best cascade (circled in red) varies as the system workload and the tolerable SLO violation ratio change.

panel plots all feasible cascade configurations in grey by varying model combinations and routing policies. The Pareto frontier<sup>1</sup> obtained by two-model and three-model cascades are colored in red and blue, respectively. Two empirical facts stand out. First, the red and blue frontiers coincide over the relevant latency range: for any latency budget, a two-model cascade attains essentially the same best FID as a three-model cascade. Second, while the blue frontier can fill in a few intermediate points (i.e., slightly finer granularity), it does not deliver significantly better quality at a given latency.

The implication is that adding a third stage offers little benefit but introduces system overhead: an extra first-stage inference pass, additional discriminator evaluations, increased queuing between stages, and more routing/placement decisions, each contributing to latency and control complexity. Given that two-model cascades already realize the tight Pareto trade-off, we adopt a two-stage design and focus our effort on adaptive model-pair selection and hybrid routing to minimize cascade cost while preserving response quality.

## 2.3 Rationale for dynamic model choice

Given that our system adopts a two-model cascade, it is natural to ask which pair of models can provide the best system performance. We empirically observe that none of the fixed lightweight/heavyweight model pairs remains optimal across varying query demands.

Figure 2-*right* shows the best two-model cascade configurations vary with the latency budget. It plots the Pareto frontier of two-model cascade configurations built from four candidates in the left panel. The orange dashed lines partition latency into three regimes. Within each regime, the

<sup>1</sup>A Pareto frontier  $P$  is a set of model cascades such that for every  $m \in P$  there is no other model cascade  $m' \in P$  that has *both* lower FID and latency than  $m$ . In that sense, all model cascades in the Pareto frontier represent an optimal tradeoff between the two objectives where one objective can be made better only at the cost of the other.

frontier points arise from a different model cascade, <SDXL-Lightning, SD3.5-Turbo> at low latency, <SD3.5-Turbo, SD3.5-Medium> at mid latency, and <SD3.5-Medium, SD3.5-Large> at high latency. We observe that different model cascades offer different latencies and response qualities. Hence, when the allowed SLO is tighter, a faster cascade is preferred to satisfy deadlines; when the SLO relaxes, cascades of higher quality can be chosen to increase the response quality.

Figure 3 further shows the best two-model cascades vary with the query loads. It compares several two-model cascades under low demand (left panel) and high demand (right panel) with the SLO held fixed. Each cascade serves queries with the resource allocation algorithm in DiffServe [5]. At low load, all pairs keep SLO violations small. <SD3.5-Turbo, SD3.5-Medium> (red star) attains the best violation rate with competitive FID, while <SD3.5-Medium, SD3.5-Large> trades a slight increase in violations for the best FID (grey diamond). Under high load, as capacity constraints surface, pairs involving slower models (i.e., grey diamond) cannot meet throughput demands and incur large violations, whereas <SDXL-Lightning, SD3.5-Turbo> (blue down-pointing triangle) remains within SLO and delivers the best quality–latency balance for that demand.

The results demonstrate that no single light/heavy pair is universally optimal. The optimal pair varies with both the latency budget and the workload, because different pairs rest on different segments of the quality-latency Pareto frontier and saturate at different throughputs. This motivates dynamic model-pair selection at runtime.

## 2.4 Rationale for hybrid query routing architecture

We argue for a hybrid query routing architecture by noting that both a router and a discriminator are needed and either one alone is insufficient, as they address complementary failure modes of the model cascade. If we want to solely use a router to evaluate the hardness of queries and route queries based on that, the router should be lightweight, introducing negligible overhead, and also accurate such that most of the queries will not be misclassified, i.e., false “hard” queries can cause unnecessary waste of GPU resources, and false “easy” queries can reduce the response quality. While query hardness has been studied in [11, 22, 38], estimating query hardness for text-to-image generation with a router is still an open and non-trivial research problem. Building a router that classifies queries with high accuracy is difficult.

A discriminator in the model cascade is usually effective in determining the hardness of a query, which is done in prior work [5, 8]. However, if we use a discriminator alone, all queries will go through the lightweight model regardless of hardness, then be evaluated by the discriminator, which brings in additional overhead, especially when the first model of the cascade requires significant computation. For instance, in Figure 2, when adopting model pair <SD3.5-Medium, SD3.5-Large>, of which the latency is  $\sim 13$ s and

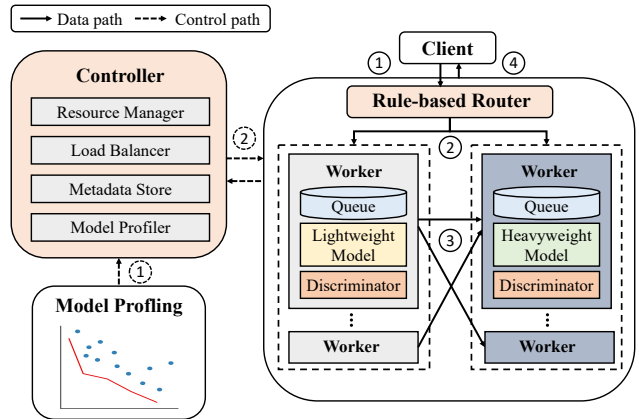


Figure 4. System Architecture of HADIS.

$\sim 27$ s respectively, the additional overhead for the first model of the cascade can be 33% of the execution latency.

We therefore adopt a hybrid architecture, combining both a router and a discriminator. The rule-based router sends obviously hard queries directly to the heavyweight model, while the rest go to the lightweight model. The discriminator then evaluates the outputs from the lightweight model and catches false “easy” cases for re-routing to heavyweight models. This design avoids unnecessary first-stage work for clearly hard queries, preserves quality by correcting router mistakes, and keeps the added control cost minimal. Our evaluation in Section 4.4 shows this hybrid routing reduces SLO violations versus discriminator-only and improves FID versus router-only, delivering the best quality-latency trade-off under identical hardware resources.

## 3 HADIS Design

We present the architecture of HADIS, a diffusion model serving system that incorporates the architectural elements presented in §2. We first provide an overview (§3.1) and then detail the main features of HADIS, including adaptive model cascading (§3.2), hybrid routing (§3.3), and resource management (§3.4).

### 3.1 Overview of HADIS

Figure 4 shows the system architecture of HADIS. It has three major components: Controller, Query Router, and Workers. We explain how these components are involved in the control path and the data path. The control path is marked with dotted arrows in Figure 4. HADIS is initialized with a set of diffusion models registered in the Controller. The control path takes mainly two actions: (1) The Controller profiles the registered models and pairwise model combinations offline to generate a cascade configuration lookup table. (2) At runtime, the Controller leverages this table to select the optimal cascade configuration. Each configuration includes a model

pair and the associated thresholds. The data path is marked with solid arrows in Figure 4. (1) A query from the client is sent to the query router. (2) The router estimates query hardness and routes the query to a worker hosting a suitable diffusion-model variant. (3) If the query is first processed by the lightweight model and the quality score of the generated response is below the threshold, the worker re-routes the query to another worker with a more heavyweight model. (4) The final output is returned to the client. We next describe each main system component.

**Controller.** A centralized Controller manages resources and coordinates system modules. The Controller includes the following components: (1) A *Resource Manager* that periodically solves MILP to determine the model pair and thresholds (i.e., the router’s *hardness threshold* and the discriminator’s *quality threshold*) and to produce a resource allocation plan (i.e., model placement across workers and batch sizes); (2) A *Load Balancer* that generates routing tables so each query is directed to a worker, and updates these tables when model selection or placement changes. (3) A *Metadata store* that periodically pulls heartbeats from the Query Router and Workers to update execution statistics, including per-model queue lengths and demand at each worker. (4) A *Model Profiler* that supplies a lookup table of profiled cascade configurations to the Resource Manager. Only registered diffusion-model pairs and discriminators are eligible for adaptive model cascading. §3.2 explains construction of the lookup table and §3.4 presents the resource-management formulation based on the lookup table.

**Workers.** Each worker maintains a local queue and processes queued queries using its hosted model. A worker hosts either a lightweight model co-located with a discriminator or a heavyweight model at any given time; this role is dynamic and can be swapped at runtime to handle time-varying demand. The Controller determines the batch size, which model variant to host, and the quality threshold for each worker, while workers report status (e.g., queries received, queue lengths, timeouts) back for planning.

**Query Router** The router sits on the data path between clients and workers. It implements a rule-based prompt analyzer that assigns obviously hard queries directly to heavyweight models and the rest to lightweight models. The rule-based analyzer is part of the hybrid routing design and will be elaborated in §3.3.

### 3.2 Adaptive Model Cascading

Adaptive model cascading dynamically selects the appropriate model pairs in a cascade given the current demand and latency SLO. However, determining both the optimal cascade and resource-allocation plan is NP-hard. The search space can be prohibitively large due to numerous model candidates, decision thresholds, model placements, and batch-size choices. HADIS addresses this challenge by decomposing the

problem into two stages: offline model profiling and online MILP-based resource management.

**Model candidate selection.** The model pool could contain many variants spanning a broad latency-quality spectrum. Exhaustively profiling all combinations is impractical. We therefore prune the pool with three heuristic, reproducible rules before any offline benchmarking. Figure 2(left) illustrates model selection from a pool. Models colored in orange are retained as candidates, while the blue ones are discarded. The three heuristic rules are:

- *Adjacency pruning.* If multiple models exhibit *similar* latency and FID, we retain a single representative and discard the others.
- *Dominance pruning.* If one model *Pareto-dominates* another (no worse in latency and strictly better in quality, or vice versa), we keep the dominating model and drop the dominated ones.
- *Intermediate redundancy.* If a model lies approximately on the *segment* between two other models that are close in latency, we omit it. In a two-stage cascade, thresholding between the neighbors can reproduce its trade-off.

**Offline profiling and lookup-table construction.** After selecting candidates, we profile two-model cascades formed by ordered pairs <lightweight, heavyweight>. For each pair we sweep the hardness threshold and quality threshold over a fixed grid. Each sweep point defines a cascade configuration, which we evaluate and record:

- *model\_pairs:* the pair instantiating the lightweight and heavyweight roles
- *diff\_thres:* the router’s hardness threshold
- *qual\_thres:* the discriminator’s quality threshold
- *route\_ratio:* the measured fraction of queries processed by each model under these thresholds
- *FID:* the resulting response quality

We then prune dominated rows to retain only Pareto-optimal configurations. The union over all pairs yields a compact lookup table of <pair, thresholds> configurations that captures the relevant quality-latency trade-offs and induced routing fractions. This table is the sole input to the online phase, where the Resource Manager selects one configuration and jointly decides model placement and batch sizes via a fast MILP, enabling HADIS to adapt model pairs and thresholds at runtime without expensive online exploration.

### 3.3 Hybrid Routing

HADIS employs: 1) a rule-based router that estimates query hardness *before* any generation, and 2) a CLIP (Contrastive Language-Image Pre-training)-based discriminator that evaluates the *generated* image. Hard queries can bypass the lightweight model, while the discriminator catches false “easy” cases after a lightweight model. The decision thresholds are tuned online by the Resource Manager in §3.4.

| Feature           | Description and Rule  |
|-------------------|---|
| Prompt length     | Longer prompts often increase hardness  |
| Token rarity      | Rare words are harder to visualize, increasing hardness   |
| Num. of objects   | A Larger number of objects in the prompt makes it harder to visualize   |
| Abstractness      | Abstract concepts (e.g., “freedom”, “hope”) are harder than concrete ones   |
| Attribute density | More modifiers increase the hardness  |
| Spatial relations | More relation counts (e.g., “in front of”, “next to”) increase compositional demand.                                    |
| Action verbs      | Dynamic scenes (e.g., “running”, “holding”) are harder than static ones   |
| Named entities    | Proper nouns may not be well-represented in training data for diffusion model (e.g., local brands), increasing hardness |

**Table 1.** Features and proposed rules of the rule-based router.

**Rule-based router.** The Query Router includes a rule-based prompt analyzer that extracts and normalizes a compact feature vector from the query prompts, computing a *hardness score* using the weighted sum. The rules that estimate hardness are designed heuristically. Table 1 lists the features and corresponding rules used in the router. The feature weights are tuned via grid search, and we select coefficients that optimize the quality-latency objective, providing evidence that misrouting is reduced.

**CLIP-based discriminator.** The Discriminator determines whether the output of the lightweight model is aesthetically acceptable. If so, the result is returned to the client, otherwise the query is re-routed to the heavyweight model. We use a CLIP backbone [28] because it provides robust image embeddings for aesthetic evaluation [16]. The discriminator keeps the pretrained CLIP frozen and fine-tunes a multi-layer perceptron (MLP) head. The model is trained to distinguish generated images from real images and then used for inference to decide whether a lightweight output meets the quality threshold.

*Training.* We train the discriminator as a binary classifier to distinguish high-quality, real images (e.g., ImageNet [30]) from images generated by our candidate diffusion models. This teaches it to detect typical divergences, such as loss of sharpness, texture incoherence, and structural glitches, enabling accurate quality assessment within the cascade.

*Inference.* Given a prompt and its generated image, CLIP produces text and visual embeddings; the MLP head consumes the visual embedding and outputs a softmax score in  $[0, 1]$ , used as the *quality score* (likelihood the image is “real-like” and thus high quality). The discriminator can also compute the CLIP score [17] (cosine similarity between visual and text embeddings) to assess semantic alignment at no extra inference cost. While we do not report semantic metrics in our evaluation because candidates differ little on

CLIP score, the signal is useful in production and can be combined with the quality score as a safety check.

**Hybrid routing with thresholds.** The *hardness threshold*  $\theta$  and *quality threshold*  $\tau$  are the keys to HADIS’s model scaling workflow, as shown in Figure 1. These parameters are co-optimized with other system settings such as model pairs and batch sizes, which are discussed at §3.4. After lightweight inference produces an image, the discriminator outputs a scalar quality score. If the score is below  $\tau$ , the query is re-routed to the heavyweight stage. Increasing  $\tau$  improves response quality but raises compute and latency as more borderline outputs are rejected and re-routed. On the other hand, obviously hard queries can bypass the lightweight stage when the router’s hardness score exceeds  $\theta$ , saving resources and latency. Increasing  $\theta$  makes the router stricter about labeling prompt “hard”, so a larger fraction of queries first pass through the lightweight stage. This may reduce average queueing at the heavyweight stage but risks higher overall system overhead if lightweight outputs subsequently fail the quality criterion determined by  $\tau$ .

### 3.4 Resource Management

The Resource Manager adapts HADIS to the current workload by jointly (i) selecting the cascade configuration, including a lightweight/heavyweight model pair and thresholds, (ii) placing models across workers, and (iii) choosing batch size per model. It tunes thresholds (i.e., the router’s hardness threshold and discriminator’s quality threshold) to balance response quality and latency as demand shifts. For instance, during low demand, a lower hardness threshold or higher quality threshold prioritizes image quality, while at peak times, a higher hardness threshold or lower quality threshold ensures fewer queries are routed to the heavyweight models, allowing minor quality compromises to meet latency deadlines. When observed demand exceeds the capacity of the current pair under its active thresholds, the Resource Manager shifts to a lighter configuration and vice versa. These changes are coordinated with model placement and batch-size updates so that workers are reallocated to match the new routing schedule and each model operates near its latency/throughput sweet spot.

**The resource management problem.** We formulate the problem with cascade configuration selection as a mixed-integer linear program (MILP) over a pre-profiled lookup table of cascade configurations (described in §3.2). At runtime, the Resource Manager selects one configuration and decides model placement and batch sizes per model so that demand is satisfied and the latency SLO is met while minimizing FID (maximizing response quality).

*Optimization variables.* For each model pair, we introduce a binary selector  $z_k$  over the threshold configuration  $k$  of that pair. A threshold configuration  $k$  includes a hardness threshold and a quality threshold (i.e.,  $k = \langle \tau, \theta \rangle$ ). For each model  $i$  in the pair, we choose an integer worker count  $x_i \geq 0$

and a one-hot batch size via binaries  $y_{i,b}$  over a discrete set of batches  $b$ . The lookup table provides the routing fraction  $r_{k,j}$  to model  $i$  under configuration  $k$ , the profiled latency  $L_{i,b}$  and throughput  $\mu_{i,b}$  at batch size  $b$ , and the quality of the configuration  $FID_k$ . Let  $\lambda$  denote the system demand,  $S$  the available workers for this pair, and  $T_{SLO}$  the latency deadline. Queuing delay for model  $i$  is estimated online from the instantaneous queue length and the arrival rate.

**Constraints.** The variables must satisfy three groups of constraints. First, considering the resource availability, each model selects a single batch size, each cascade has exactly one threshold configuration for the pair, and worker usage is bounded by the budget:

$$\sum_b y_{i,b} = 1, \quad \sum_k z_k = 1, \quad \sum_i x_i \leq S \quad \forall i \quad (1)$$

Second, considering the throughput constraint, per-model capacity must cover the share of demand routed to that model under the chosen configuration:

$$x_i \sum_b y_{i,b} \mu_{i,b} \geq \lambda \sum_k z_k r_{k,i} \quad \forall i \quad (2)$$

Then, considering the latency constraint, end-to-end latency must remain within the SLO. Let the selected batch latency for model  $i$  be  $\widehat{L}_i = \sum_b y_{i,b} L_{i,b}$  and let  $D_i^{\text{queue}} = \alpha \frac{Q_i}{\lambda_i}$  denote the queuing delay estimate given Little’s law [34] where  $\alpha$  is a safety factor. We impose a conservative path bound, making sure the latency constraint is met:

$$\sum_i (\widehat{L}_i + D_i^{\text{queue}}) \leq T_{SLO} \quad (3)$$

Eventually, the objective quality variable equals the FID of the selected configuration:

$$F = \sum_k z_k FID_k \quad (4)$$

**MILP formulation.** The resource manager identifies the optimal configuration and allocation by

$$\min_{\{z_k\}, \{x_i\}, \{y_{i,b}\}, \{u_{i,b}\}} F \quad \text{s.t. Eqs. (1)–(4)} \quad (5)$$

**Solving the MILP.** The optimization problem is solved periodically by invoking an MILP solver to identify a global optimal cascade configuration, model allocation, and model batch sizes. We estimate query demand  $\lambda$  using an exponentially weighted moving average (EWMA) on the recent demand history. Note that the time overhead to solve the MILP does not lie on the critical path of query serving as the MILP is called asynchronously. We provide a detailed analysis of the overhead in Section 4.8.

## 4 Evaluation

This section evaluates the efficacy of HADIS. We first outline the common experimental setup (§4.1). We then present end-to-end results and analysis of system performance on real-world workloads (§4.2) and synthetic workloads (§4.3). We

quantify the benefit of hybrid routing and the effectiveness of MILP-based resource allocator via controlled ablation studies (§4.4 and §4.5). We study sensitivity of HADIS to various latency SLOs (§4.6) and to workload hardness composition of queries (§4.7). Finally, we report the runtime overheads of each system component (§4.8).

### 4.1 Experiment settings

**Implementation of HADIS.** We implement HADIS on a testbed cluster to evaluate performance on real GPU hardware. The system implementation consists of ~5K lines of Python code. We use the HuggingFace [35] and PyTorch frameworks [25] to execute the diffusion models and discriminator, and use spaCy [19] to extract prompt features for the rule-based query router. Our cluster consists of 16 workers with NVIDIA L40S GPU, and system components including Controller, Load Balancer, Worker, and Client, communicate via gRPC for low-latency coordination. We use Gurobi [15] to solve our MILP optimization. Unless otherwise noted, all results reported in this paper are collected on this testbed.

**Model Selection.** We apply our model-selection rules to choose four diffusion models that provide diverse latency-quality trade-offs, including SDXL-Lightning, SD3.5-Turbo, SD3.5-Medium, and SD3.5-Large. SDXL-Lightning [21] is a fast generative model that produces an image in a few steps; in our setup, we use 2 steps, yielding ~0.5s latency per 1024×1024 image on an L40S GPU. Stable Diffusion 3.5 [6] is a diffusion transformer family that can produce images of high quality. We configure SD3.5-Turbo with 4 steps (~1.3s per image on L40S), while SD3.5-Medium and SD3.5-Large use 50 steps, with latencies of ~13s and ~27s, respectively, on the same hardware. Unless otherwise noted, the latency SLO is 60s, chosen as a multiple of the slowest model’s runtime, and all models render at 1024×1024 resolution.

**Datasets and workloads.** For quality evaluation, we use *ImageNet-1k*, a widely-used subset of ImageNet [30], with associated captions. We take the first 5k caption-image pairs, using captions as prompts and the corresponding images as the reference set for FID computation. To drive system load, we use the Microsoft Azure Functions trace [32] as a representative real-world workload, applying shape-preserving scaling to match our cluster’s capacity.

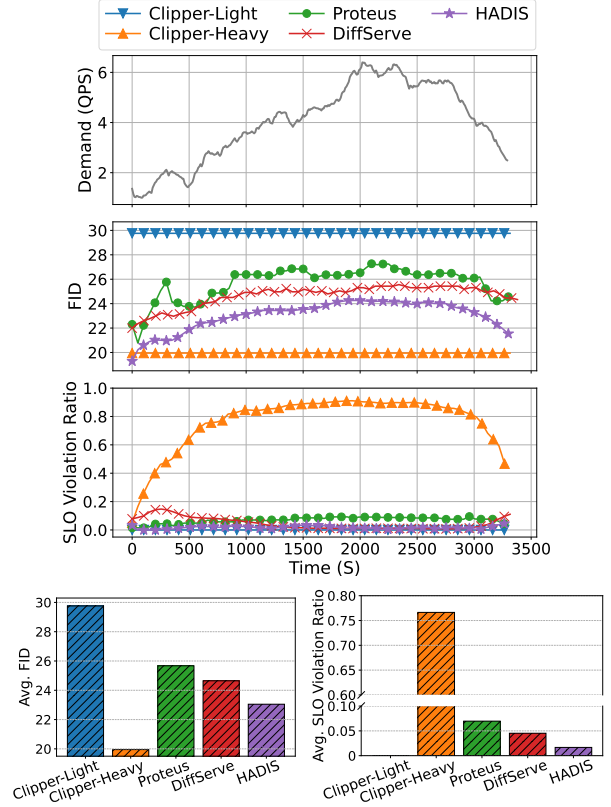
**Evaluation Metrics.** We assess system performance using two primary metrics. (1) *Response quality FID* measures the distance between the distribution of generated images and a reference set of real images (lower is better). For each system configuration, we run all queries through the system and compute FID against the reference images from our evaluation set to evaluate the quality of generated images. (2) *SLO violation ratio* is the fraction of queries whose end-to-end latency exceeds the latency deadline or are proactively dropped because they are predicted to miss it.

**Baselines.** We compare HADIS against a spectrum of baselines ranging from fully static (Clipper) to dynamic resource allocation (Proteus) and query-aware cascading (DiffServe).

- **Clipper** [9] is a static baseline, which does not dynamically select models or allocate resources, and cannot route queries given query complexity. We implement two versions of Clipper, **Clipper-Light**, minimizing SLO violations with the most lightweight model (SDXL-Lightning), and **Clipper-Heavy**, maximizing response quality with the most heavyweight model (SD3.5-Large). Note that Clipper is also representative of other static inference-serving systems, such as TensorFlow-Serving [23], which depend on the application developer to handle the resource allocation of models.
- **Proteus** [4] is a high-throughput serving system that selects among multiple model variants as workload changes. It scales quality by switching to faster variants from the four diffusion model candidates under high load and switching to higher-quality variants when capacity allows. Proteus runs single-stage inference without a per-query cascade or discriminator, where queries are randomly routed to each worker with equal probability.
- **DiffServe** [5] is a text-to-image serving system built around a model-cascading pipeline. DiffServe uses an MILP planner to adapt to demand by jointly setting resource allocations and the quality threshold of the discriminator. Unlike HADIS, it employs a fixed pair of light and heavyweight models. In our implementation, we fix the pair to SD3.5-Turbo and SD3.5-Large, which outperformed other pairings on the query workload.

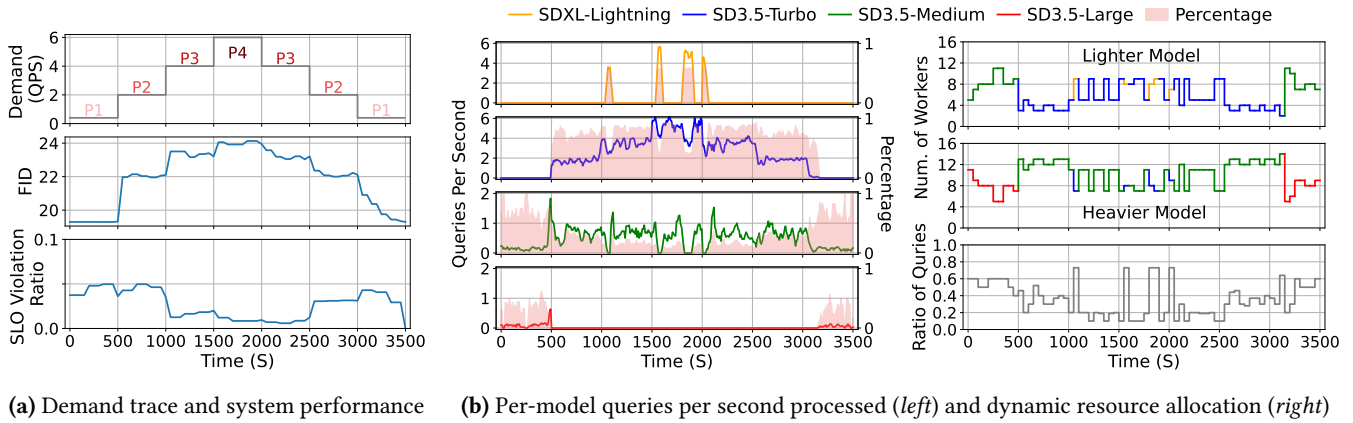
#### 4.2 Performance on Real-World Traces

Figure 5 reports time series of demand, FID, and SLO violations, plus their averages over the trace. Clipper-Light has the lowest quality (highest FID) and low violations because it processes all queries with the fastest model Clipper-Heavy uses the highest-quality model, achieving the best FID among baselines but incurring significant violations (up to 90% at peak, 77% on average). Proteus dynamically tunes the resource allocation according to demand changes, selecting higher-quality models under low load and shifting toward faster models under high load. However, as it is query-agnostic, in which all queries are routed to the same model with equal probability, easy queries could be over-served by heavy models while hard queries could be under-served by light models, thus its quality improvement over Clipper-Light is limited and suffers from high SLO violations (up to 12% during the peak, 7% on average). DiffServe offers a better response quality and a lower SLO violation ratio due to its dynamic resource allocation and query-awareness. It routes queries to the heavyweight model given the decision made by the discriminator, thus improving the quality over Proteus by up to 12% in the timeseries and 4% on average.



**Figure 5.** End-to-end comparison on real-world traces. On average, HADIS achieves a 7-23% reduction in FID compared to baselines except Clipper-Heavy, and reduces SLO violation by 2.7 $\times$ , 4.2 $\times$ , and 45 $\times$  compared to DiffServe, Proteus, and Clipper-Heavy. Clipper-Light’s avg. SLO violation is zero.

HADIS offers the best performance as it couples query-aware routing, adaptive model selection, and MILP-based resource allocation, choosing the best pair of models with routing thresholds, and allocating GPU resources given the current workload. As demand rises, it shifts traffic toward faster model cascade variants and tightens usage of heavyweight models to protect latency; as demand decreases, it reallocates GPUs to model cascade variants with better response quality and relaxes thresholds to recover quality. Consequently, HADIS improves quality by up to 10%-35% over baselines while maintaining low violations. During peak, it offers better quality than all baselines except Clipper-Heavy, which yields significantly high SLO violations. As shown in the average statistics, HADIS achieves a 7%-23% reduction in FID compared to baselines, and reduces the average SLO violation ratio by 2.7 $\times$ , 4.2 $\times$ , and 45 $\times$  compared to DiffServe, Proteus, and Clipper-Heavy.



**Figure 6.** Performance of HADIS on synthetic traces. (a) Time-series of a piecewise-constant demand trace and system performance. **Top:** demand QPS with four phases (P1-P4). **Middle:** FID rises when demand increases and recovers as demand decreases. **Bottom:** SLO violation ratio stays low overall, with brief decreases during P3/4 and increases during P1/2 due to the latency of models in use. (b) **Left:** queries are shifted toward faster variants under higher load and back toward higher-quality variants as load decreases. **Right:** number of workers assigned to lightweight/heavyweight models is coordinated with the ratio of queries routed to heavyweight models to maintain low SLO violations while maximizing quality as demand fluctuates.

### 4.3 Performance on Synthetic Traces

This section evaluates HADIS on a controlled synthetic workload and explains how the system adapts its routing, model selection, and resource plan over time (Figure 6).

We replay a piecewise-constant demand trace with four load levels (P1-P4) arranged as rising, peak, and falling phases. Each level is held long enough for the system to settle before the next step change. This shape mimics bursty traffic to evaluate the responsiveness of resource allocation under both load increases and decreases. Across all phases, HADIS adapts to workload changes dynamically, yielding high response quality with low SLO violations.

In Figure 6a, as demand climbs to P3/P4, FID increases modestly, representing response quality decreases; when demand falls back to P2/P1, response quality (FID) improves. HADIS trades some quality for higher throughput under high load and recovers quality when capacity returns. Throughout the time-varying demands, the SLO violation ratios remain low (1%~5%). Notably, SLO violations are relatively high during P1/P2 because the models in use are mainly SD3.5-Large and SD3.5-Medium, as shown in Figure 6b, which have long execution latency in return for higher quality, leading to higher SLO violation rates.

In Figure 6b-left, we can observe per-model throughputs (processed queries per second, QPS) and percentages of queries shared by each model. The traffic mix shifts toward faster models (i.e., SDXL-Lightning and SD3.5-Turbo) during P3/P4 and back toward higher-quality models (i.e., SD3.5-Medium and SD3.5-Large) during P1. This is because the MILP chooses model combinations from the profiled table that meet the active SLO under the current load. When QPS

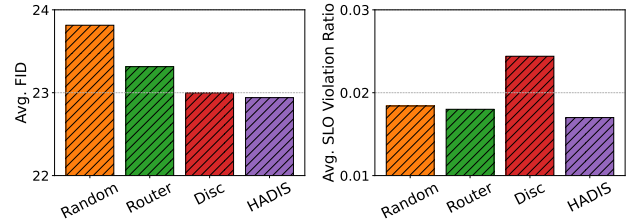


**Figure 7.** Effectiveness of hybrid routing. The hybrid routing (HADIS) outperforms Random and Router-only (Router) in FID and reduces SLO violations compared to Discriminator-only (Disc), achieving the best quality-latency trade-off under identical resources.

rises, HADIS responds by adjusting the hardness and quality threshold to reduce the fraction of query re-routing, leading to an increased percentage of queries on lightweight paths. The observation is more obvious in Figure 6b-right, which shows the GPU workers allocated and the ratio of queries routed to the heavyweight model. Note that in P3 and P4, HADIS is able to achieve high quality with heavier models while meeting latency SLO, because SDXL-Lightning is applied periodically to drain the queued queries accumulated by those models, preventing timeouts.

### 4.4 Effectiveness of Hybrid Routing

We now show an ablation study of our hybrid routing approach in Figure 7 to understand the effect of the rule-based router and the image discriminator. We isolate the routing policy by running four variants: (1) **Random:** we randomly assign hardness and quality scores to each query, using these

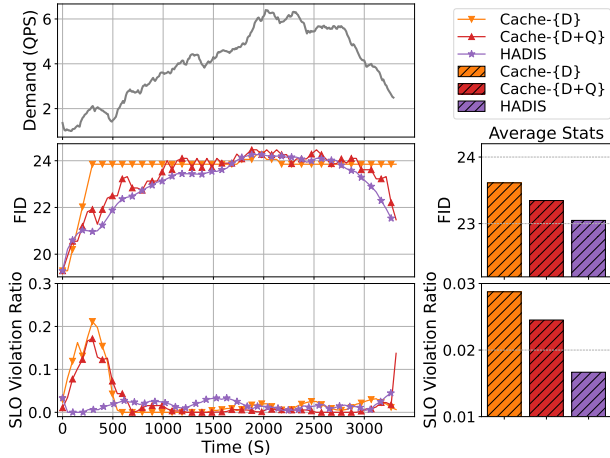


**Figure 8.** Comparison of resource allocation strategies. **HADIS** applies MILP. **Cache-{D}** caches plans using demands as key; **Cache-{D+Q}** caches plans using demands and queue length as key. Cached policies lag during load shifts, showing transient quality drops and violation spikes, whereas **HADIS** adapts in real time, yielding lower violations with comparable or better FID.

random scores for routing decision making. (2) **Router-only**: the routing decisions are made by the rule-based router only without discriminator-based re-routing. (3) **Discriminator-only**: the routing decisions are made by the discriminator only without the router. (4) **HADIS**: hybrid routing is enabled with both rule-based query routing and discriminator-based re-routing. All variants are evaluated on the same real-world trace with the same MILP-based resource allocator.

Figure 7 shows that **HADIS** achieves the lowest average FID and the lowest SLO violation ratio across all variants. Random and Router-only suffer from worse FID at similar SLO violation levels since *hard* queries are served by light-weight models due to misclassification. Discriminator-only improves FID but suffers from higher violations, as it forces every query through the light model, paying extra latency. In contrast, **HADIS** adopts hybrid routing, combining query-aware rules to skip the light stage for obviously hard queries and a learned discriminator to catch false “easy” cases, while adjusting thresholds to match workload. Thus, it preserves low latency and achieves higher response quality.

#### 4.5 Evaluation of Resource Allocation

We ablate the resource planner by implementing two variants, **Cache-{D+Q}** and **Cache-{D}**. Unlike **HADIS** which solves an online MILP to seek optimal resource allocation plans at runtime, these cached planners select and apply a previously computed resource allocation configuration on a cache hit. **Cache-{D}** stores plans in a lookup table keyed by a discretized *range* of system demand, whereas **Cache-{D+Q}** uses a two-dimensional key composed of a *range* of system

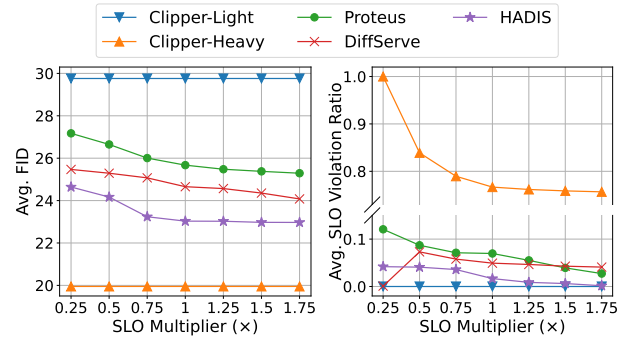


**Figure 9.** Sensitivity to latency SLO on **HADIS** and baselines. **HADIS** guarantees low SLO violations and high quality over varying SLO values across all methods.

demand and a *range* of worker queue length. At runtime, we quantize the observed demand (and queue length for **Cache-{D+Q}**) to their respective ranges and probe the table. If the measurements fall within any keyed range that has an associated plan, we declare a cache hit and apply that plan. If not, we solve the MILP to obtain a plan and then insert it into the lookup table under the corresponding range key.

Figure 8 shows the timeseries results and average statistics. **Cache-{D}** performs the worst, where high FID and SLO violation spikes early in the run were observed. The planner lags during load shifts as it is agnostic about the real-time system workload. **Cache-{D+Q}** is more responsive than **Cache-{D}** by capturing congestion through the extra key dimension in the lookup table. We empirically observe that both caching variants exhibit a startup spike in SLO violations since their selected plans are either biased or unsynchronized with the actual real-time demands. Once the workload settles, violations stabilize for both variants.

Unlike the cached plans that react only when the key changes, **HADIS** with online MILP adapts plans in real time, rebalancing workers and thresholds as demand changes. It prevents prolonged queue growth and keeps low violations while maintaining comparable or better FID, avoiding under- or over-provision when workload fluctuates.

The results also reveal the potential of caching. Moving from **Cache-{D}** to **Cache-{D+Q}** improves both FID and SLO violation ratio, suggesting that better keys help. A hybrid planner using MILP online to correct mismatches and to populate a cache could deliver MILP-level performance with lower optimization overhead, improving scalability for large-scale deployments.

#### 4.6 Sensitivity to Latency SLO

We change the SLO multiplier from  $0.25\times$  to  $1.75\times$  to modify the latency SLO, and run **HADIS** and baselines on the real-world trace. The average FID and SLO violation ratio of all methods is reported in Figure 9.

As the SLO relaxes, all methods improve on both FID and SLO violations, but HADIS outperforms baselines across the entire range. Under tight budgets (0.25-0.75 $\times$ ), HADIS sustains low violations while achieving lower FID than Proteus and DiffServe (up to 11% and 7%). Clipper-Light maintains  $\sim 0$  violations but delivers the worst FID, whereas Clipper-Heavy attains the best FID yet exhibits very high SLO violation ratios even with higher SLO values. Note that the SLO violation ratio of DiffServe is nearly zero at the 0.25 $\times$  SLO multiplier because the latency SLO (15s) is lower than the execution time of the heavyweight model ( $\sim 27$ s), making the MILP allocate all workers to lightweight models. Although HADIS could also select a lighter cascade, sacrificing some FID for near-zero SLO violations, it would violate HADIS’s objective of maximizing quality under SLO constraints. Thus, the planner avoids such degenerate allocations. For SLO multipliers above 1 $\times$ , all methods become demand-bound rather than deadline-bound, where performance is limited by the offered QPS. Results show that HADIS guarantees low SLO violations and high quality over a broad range of SLO values.

#### 4.7 Sensitivity to Hardness of Queries

We study how sensitive HADIS is to shifts in the hardness distribution of incoming queries. We isolate the effect of hardness from demand by fixing the query demand and constructing a four-phase trace: the first and third phases contain only *Easy* queries, and the second and fourth contain only *Hard* queries. Queries are categorized using weighted scores over textual features. As shown in Figure 10, during Easy phases, the system settles into a relatively dynamic phase where the lightweight model serves the majority of traffic. Immediately after each transition to a Hard phase, the router bypasses lightweight inference for a larger fraction of queries, sharply increasing the heavy-class intake. The heavy queue rises, triggering workers assigned to the heavyweight model. These results confirm that HADIS adaptively concentrates resources on heavyweight models precisely when hard queries predominate, highlighting the value of our query-side bypass design.

#### 4.8 Overhead Analysis

HADIS introduces three sources of overhead: (1) a query router that performs rule-based feature extraction and a score computation (5ms per query), (2) a CLIP-based discriminator that computes quality score for generated images (7ms per query on an L40S GPU), and (3) an MILP-based resource allocator whose measured average runtime is  $\sim 30$ ms per planning cycle. The aggregated overhead of router and discriminator is  $\sim 12$ ms, which is negligible relative to diffusion inference of SDXL-Lightning (2.4%), SD3.5-Turbo (0.9%), SD3.5-Medium (0.01%), and SD3.5-Large ( $< 0.01\%$ ). Moreover, since the MILP solver runs periodically and applies updates asynchronously, this overhead is off the critical path and does not affect individual queries.

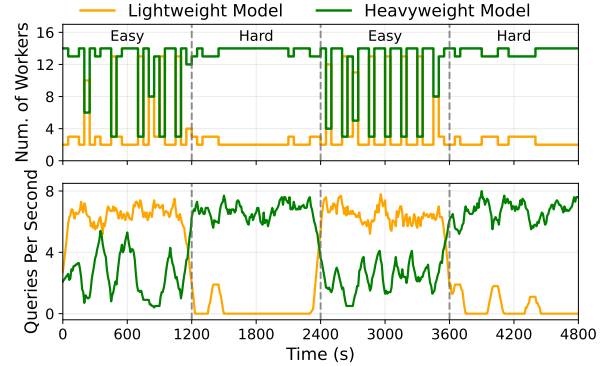


**Figure 10.** Sensitivity to Query Hardness. HADIS adaptively bypasses lightweight inference and reallocates workers according to query complexity.

## 5 Related Work

Model serving systems aim to provide a unified abstraction to the user, hiding details of the underlying ML frameworks, data preprocessing, and performance optimization. Representative production systems include SageMaker [31], Triton [1], TensorFlow Serving [3], and TorchServe [2], whereas research prototypes include Nexus [33], BATCH [7], and Clockwork [12]. While mature and widely deployed, these systems typically require users to specify the models and then handle resource management based on the user-specified models. Without reasoning about multiple model variants for the same task, such framework gives up opportunities to further balance accuracy, latency, and cost. Some recent systems improve upon it by managing both resources and model variants. For instance, Clipper [10], Rafiki [36], and Cocktail [13] use model ensembles to enhance response quality. INFaaS [29], Model Switching [39], and Sommelier [14] adaptively select model variants in response to system loads. Proteus [4] exploits accuracy–efficiency trade-offs across model variants to meet throughput requirements while maximizing accuracy. Still, systems that primarily react to system state and ignore query difficulty miss optimization opportunities when requests vary in semantic complexity. A cascading architecture for large language model (LLM) serving has therefore been proposed, such as CascadeBERT [20] and Tabi [37]. These systems allow easy queries to be processed exclusively by light models and decide whether to return results or re-route inputs to more complex models. DiffServe [5] constructs diffusion model cascades and frames resource allocation as a mixed integer linear programming (MILP) problem to optimize both the efficiency and response quality. Still, the cascading frameworks that fixes the cascade pair and always initiates with a lightweight model pass can waste compute of re-routing difficult prompts. HADIS improves upon above frameworks by adaptively selecting the optimal model pair and decision thresholds based on the time-varying query demands. Unnecessary lightweight

inference is also avoided by sending obviously hard prompts directly to heavyweight models.

## 6 Conclusion

We presented HADIS, a diffusion model serving system that couples adaptive model cascading with hybrid routing and a lookup-table-driven MLP planner to meet latency SLOs while delivering high response quality. HADIS profiles candidate model pairs offline to build Pareto-optimal cascade configurations, then selects the best pair and thresholds online while jointly allocating GPUs and batch sizes. A rule-based router and a CLIP-based discriminator work in tandem to preemptively route clearly hard queries and validate outputs from lightweight models, reducing cascade overhead without sacrificing quality. Evaluated on real-world workload traces, HADIS outperforms state-of-the-art baselines, improving response quality and reducing SLO violations.

## References

- [1] 2022. *Triton inference server*. <https://developer.nvidia.com/dynamo>
- [2] 2023. *Torchserve*. <https://docs.pytorch.org/serve/>
- [3] 2024. *Tensorflow serving*. <https://www.tensorflow.org/tfx/guide/serving>
- [4] Sohaib Ahmad, Hui Guan, Brian D Friedman, Thomas Williams, Ramesh K Sitaraman, and Thomas Woo. 2024. Proteus: A High-Throughput Inference-Serving System with Accuracy Scaling. In *Proceedings of the 29th ACM International Conference on Architectural Support for Programming Languages and Operating Systems, Volume 1*. 318–334.
- [5] Sohaib Ahmad, Qizheng Yang, Haoliang Wang, Ramesh K. Sitaraman, and Hui Guan. 2025. DiffServe: Efficiently Serving Text-to-Image Diffusion Models with Query-Aware Model Scaling. *arXiv:2411.15381 [cs.DC]* <https://arxiv.org/abs/2411.15381>
- [6] Stability AI. 2024. *Introducing Stable Diffusion 3.5*. <https://stability.ai/news/introducing-stable-diffusion-3-5>
- [7] Ahsan Ali, Riccardo Pinciroli, Feng Yan, and Evgenia Smirni. 2020. Batch: Machine learning inference serving on serverless platforms with adaptive batching. In *SC20: International Conference for High Performance Computing, Networking, Storage and Analysis*. IEEE, 1–15.
- [8] Lingjiao Chen, Matei Zaharia, and James Zou. 2023. Frugalgpt: How to use large language models while reducing cost and improving performance. *arXiv preprint arXiv:2305.05176* (2023).
- [9] Daniel Crankshaw, Xin Wang, Guilio Zhou, Michael J Franklin, Joseph E. Gonzalez, and Ion Stoica. 2017. Clipper: A Low-Latency Online Prediction Serving System. In *14th USENIX Symposium on Networked Systems Design and Implementation (NSDI 17)*. USENIX Association, Boston, MA, 613–627. <https://www.usenix.org/conference/nsdi17/technical-sessions/presentation/crankshaw>
- [10] Daniel Crankshaw, Xin Wang, Guilio Zhou, Michael J Franklin, Joseph E Gonzalez, and Ion Stoica. 2017. Clipper: A {Low-Latency} online prediction serving system. In *14th USENIX Symposium on Networked Systems Design and Implementation (NSDI 17)*. 613–627.
- [11] Maria-Teresa De Rosa Palmi and Eva Cetinic. 2025. Exploring Language Patterns of Prompts in Text-to-Image Generation and Their Impact on Visual Diversity. In *Proceedings of the 2025 ACM Conference on Fairness, Accountability, and Transparency (FAccT '25)*. Association for Computing Machinery, New York, NY, USA, 2318–2348. doi:10.1145/3715275.3732158
- [12] Arpan Gujarati, Reza Karimi, Safya Alzayat, Wei Hao, Antoine Kaufmann, Ymir Vigfusson, and Jonathan Mace. 2020. Serving {DNNs} like clockwork: Performance predictability from the bottom up. In *14th USENIX Symposium on Operating Systems Design and Implementation (OSDI 20)*. 443–462.
- [13] Jashwant Raj Gunasekaran, Cyan Subhra Mishra, Prashanth Thinnakaran, Bikash Sharma, Mahmut Taylan Kandemir, and Chita R Das. 2022. Cocktail: A multidimensional optimization for model serving in cloud. In *19th USENIX Symposium on Networked Systems Design and Implementation (NSDI 22)*. 1041–1057.
- [14] Peizhen Guo, Bo Hu, and Wenjun Hu. 2022. Sommelier: Curating DNN models for the masses. In *Proceedings of the 2022 International Conference on Management of Data*. 1876–1890.
- [15] Gurobi. 2024. . <https://www.gurobi.com/>
- [16] Simon Hentschel, Konstantin Kobs, and Andreas Hotho. 2022. CLIP knows image aesthetics. *Frontiers in Artificial Intelligence* Volume 5 - 2022 (2022). doi:10.3389/frai.2022.976235
- [17] Jack Hessel, Ari Holtzman, Maxwell Forbes, Ronan Le Bras, and Yejin Choi. 2021. CLIPScore: A Reference-free Evaluation Metric for Image Captioning. In *Proceedings of the 2021 Conference on Empirical Methods in Natural Language Processing*, Marie-Francine Moens, Xuanjing Huang, Lucia Specia, and Scott Wen-tau Yih (Eds.). Association for Computational Linguistics, Online and Punta Cana, Dominican Republic, 7514–7528. doi:10.18653/v1/2021.emnlp-main.595
- [18] Martin Heusel, Hubert Ramsauer, Thomas Unterthiner, Bernhard Nessler, and Sepp Hochreiter. 2017. GANs trained by a two time-scale update rule converge to a local nash equilibrium. In *Proceedings of the 31st International Conference on Neural Information Processing Systems (Long Beach, California, USA) (NIPS'17)*. Curran Associates Inc., Red Hook, NY, USA, 6629–6640.
- [19] Matthew Honnibal, Ines Montani, Sofie Van Landeghem, and Adriane Boyd. 2020. spaCy: Industrial-strength Natural Language Processing in Python. (2020). doi:10.5281/zenodo.1212303
- [20] Lei Li, Yankai Lin, Deli Chen, Shuhuai Ren, Peng Li, Jie Zhou, and Xu Sun. 2020. Cascadebert: Accelerating inference of pre-trained language models via calibrated complete models cascade. *arXiv preprint arXiv:2012.14682* (2020).
- [21] Shanchuan Lin, Anran Wang, and Xiao Yang. 2024. SDXL-Lightning: Progressive Adversarial Diffusion Distillation. *arXiv:2402.13929 [cs.CV]* <https://arxiv.org/abs/2402.13929>
- [22] Vivian Liu and Lydia B Chilton. 2022. Design Guidelines for Prompt Engineering Text-to-Image Generative Models (*CHI '22*). Association for Computing Machinery, New York, NY, USA, Article 384, 23 pages. doi:10.1145/3491102.3501825
- [23] Christopher Olston, Fangwei Li, Jeremiah Harmsen, Jordan Soyke, Kiril Gorovoy, Li Lao, Noah Fiedel, Sukriti Ramesh, and Vinu Rajashekhar. 2017. TensorFlow-Serving: Flexible, High-Performance ML Serving. In *Workshop on ML Systems at NIPS 2017*.
- [24] OpenAI. 2023. DALL-E3. <https://openai.com/dall-e>. Accessed: July 2025.
- [25] Adam Paszke, Sam Gross, Francisco Massa, Adam Lerer, James Bradbury, Gregory Chanan, Trevor Killeen, Zeming Lin, Natalia Gimelshein, Luca Antiga, Alban Desmaison, Andreas Köpf, Edward Yang, Zach DeVito, Martin Raison, Alykhan Tejani, Sasank Chilamkurthy, Benoit Steiner, Lu Fang, Junjie Bai, and Soumith Chintala. 2019. PyTorch: An Imperative Style, High-Performance Deep Learning Library. *arXiv:1912.01703 [cs.LG]* <https://arxiv.org/abs/1912.01703>
- [26] William Peebles and Saining Xie. 2023. Scalable Diffusion Models with Transformers. *arXiv:2212.09748 [cs.CV]* <https://arxiv.org/abs/2212.09748>
- [27] Dustin Podell, Zion English, Kyle Lacey, Andreas Blattmann, Tim Dockhorn, Jonas Müller, Joe Penna, and Robin Rombach. 2023. Sdxl: Improving latent diffusion models for high-resolution image synthesis. *arXiv preprint arXiv:2307.01952* (2023).

- [28] Alec Radford, Jong Wook Kim, Chris Hallacy, Aditya Ramesh, Gabriel Goh, Sandhini Agarwal, Girish Sastry, Amanda Askell, Pamela Mishkin, Jack Clark, Gretchen Krueger, and Ilya Sutskever. 2021. Learning Transferable Visual Models From Natural Language Supervision. arXiv:2103.00020 [cs.CV] <https://arxiv.org/abs/2103.00020>
- [29] Francisco Romero, Qian Li, Neeraja J Yadwadkar, and Christos Kozyrakis. 2021. {INFaaS}: Automated model-less inference serving. In *2021 USENIX Annual Technical Conference (USENIX ATC 21)*. 397–411.
- [30] Olga Russakovsky, Jia Deng, Hao Su, Jonathan Krause, Sanjeev Satheesh, Sean Ma, Zhiheng Huang, Andrej Karpathy, Aditya Khosla, Michael Bernstein, Alexander C. Berg, and Li Fei-Fei. 2015. ImageNet Large Scale Visual Recognition Challenge. *International Journal of Computer Vision (IJCV)* 115, 3 (2015), 211–252. doi:10.1007/s11263-015-0816-y
- [31] Amazon SageMaker. 2020. Build, train, and deploy machine learning models at scale.
- [32] Mohammad Shahrads, Rodrigo Fonseca, Íñigo Goiri, Gohar Chaudhry, Paul Batum, Jason Cooke, Eduardo Laureano, Colby Tresness, Mark Russinovich, and Ricardo Bianchini. 2020. Serverless in the wild: Characterizing and optimizing the serverless workload at a large cloud provider. In *2020 USENIX Annual Technical Conference (USENIX ATC 20)*. 205–218.
- [33] Haichen Shen, Lequn Chen, Yuchen Jin, Liangyu Zhao, Bingyu Kong, Matthai Philipose, Arvind Krishnamurthy, and Ravi Sundaram. 2019. Nexus: A GPU cluster engine for accelerating DNN-based video analysis. In *Proceedings of the 27th ACM Symposium on Operating Systems Principles*. 322–337.
- [34] John F Shortle, James M Thompson, Donald Gross, and Carl M Harris. 2018. *Fundamentals of queueing theory*. Vol. 399. John Wiley & Sons.
- [35] Patrick von Platen, Suraj Patil, Anton Lozhkov, Pedro Cuenca, Nathan Lambert, Kashif Rasul, Mishig Davaadorj, Dhruv Nair, Sayak Paul, William Berman, Yiyi Xu, Steven Liu, and Thomas Wolf. 2022. Diffusers: State-of-the-art diffusion models. <https://github.com/huggingface/diffusers>.
- [36] Wei Wang, Sheng Wang, Jinyang Gao, Meihui Zhang, Gang Chen, Teck Khim Ng, and Beng Chin Ooi. 2018. Rafiki: Machine learning as an analytics service system. *arXiv preprint arXiv:1804.06087* (2018).
- [37] Yiding Wang, Kai Chen, Haisheng Tan, and Kun Guo. 2023. Tabi: An efficient multi-level inference system for large language models. In *Proceedings of the Eighteenth European Conference on Computer Systems*. 233–248.
- [38] Xing Xing, Yi Zhang, and Mei Han. 2010. Query difficulty prediction for contextual image retrieval. In *Proceedings of the 32nd European Conference on Advances in Information Retrieval (Milton Keynes, UK) (ECIR'2010)*. Springer-Verlag, Berlin, Heidelberg, 581–585. doi:10.1007/978-3-642-12275-0\_52
- [39] Jeff Zhang, Sameh Elnikety, Shuayb Zarar, Atul Gupta, and Siddharth Garg. 2020. {Model-Switching}: Dealing with fluctuating workloads in {Machine-Learning-as-a-Service} systems. In *12th USENIX Workshop on Hot Topics in Cloud Computing (HotCloud 20)*.